JACS
JOURNAL OF THE AMERICAN CHEMICAL SOCIETY

COMMUNICATION

pubs.acs.org/JACS

Preparation of Monodisperse Silicon Nanocrystals Using Density Gradient Ultracentrifugation

Melanie L. Mastronardi,[†] Frank Hennrich,[‡] Eric J. Henderson,[†] Florian Maier-Flaig,[§] Carolin Blum,[‡] Judith Reichenbach,[‡] Uli Lemmer,[§] Christian Kübel,[‡,∥] Di Wang,[‡,∥] Manfred M. Kappes,[‡,⊥,#] and Geoffrey A. Ozin*[,†]

[†]Department of Chemistry, University of Toronto, 80 St. George Street, Toronto, Ontario, Canada M5S 3H6

[‡]Institute of Nanotechnology, Karlsruhe Institute of Technology, 76344 Eggenstein-Leopoldshafen, Germany

[§]Light Technology Institute, Karlsruhe Institute of Technology, 76133 Karlsruhe, Germany

[∥]Karlsruhe Nano Micro Facility, Karlsruhe Institute of Technology, 76366 Eggenstein-Leopoldshafen, Germany

[⊥]DFG Center for Functional Nanostructures, 76028 Karlsruhe, Germany

[#]Institute of Physical Chemistry, Karlsruhe Institute of Technology, 76133 Karlsruhe, Germany

Supporting Information

ABSTRACT: We report the preparation of monodisperse silicon nanocrystals (ncSi) by size-separation of polydisperse alkyl-capped ncSi using organic density gradient ultracentrifugation. The ncSi were synthesized by thermal processing of trichlorosilane-derived sol−gel glasses followed by HF etching and surface passivation with alkyl chains and were subsequently fractionated by size using a self-generating density gradient of 40 wt % 2,4,6-tribromotoluene in chlorobenzene. The isolated monodisperse fractions were characterized by photoluminescence spectroscopy and high-angle annular dark-field scanning transmission electron microscopy and determined to have polydispersity index values between 1.04 and 1.06. The ability to isolate monodisperse ncSi will allow for the quantification of the size-dependent structural, optical, electrical, and biological properties of silicon, which will undoubtedly prove useful for tailoring property-specific optoelectronic and biomedical devices.

Semiconductor nanocrystals possess optical and electronic properties that vary predictably with crystal size, making them useful materials for tailoring optoelectronic and biomedical devices with specific optical, electrical, and biological requirements. In particular, quantum-confinement effects result in a widening of the electronic band gap and a blue shift in the photoluminescence (PL) as the particle size decreases. As a result, the archetypical II−VI and IV−VI nanocrystals (quantum dots) show great promise in optoelectronic[1,2] and biomedical[3,4] devices, including lasers, light-emitting diodes, photodetectors, next-generation solar cells, and diagnostic, therapeutic, and imaging reagents, but concerns exist over the toxicity of these materials and their effect on human health and the environment.[5,6] Therefore intense research continues on the development of alternative materials.

In 1990, Canham reported the first efficient room-temperature light emission from silicon, ultimately attributed to nanocrystalline domains in porous silicon.[7] Efficient alternative methods for the synthesis of silicon nanocrystals (ncSi) have since emerged, including annealing of SiO_x powders followed by etching with HF, plasma synthesis, and solution reduction of $SiCl_4$.[8−10] However, these synthetic methods produce samples with considerable size polydispersity. A monodisperse sample of ncSi is needed to obtain a definitive characterization of size-dependent optical, electrical, biological, and toxicological properties as well as to construct the uniform nanocrystal assemblies required for efficient state-of-the-art applications, as non-negligible nanocrystal size distributions lead to inhomogeneous broadening of spectral features and averaging effects in biomedical applications and cytotoxicity studies. Various methods have been demonstrated for postsynthetic size-selective separations of nanomaterials,[11−13] including size distribution narrowing and emission color separations of ncSi;[8,14] however, the preparation of monodsiperse ncSi using size-separation methods is still in its infancy, and therefore, information regarding the definite size-dependent properties of silicon is incomplete. The low cost and minimal cytotoxicity of silicon[15] relative to II−VI and IV−VI materials give ncSi great potential to have a significant impact in optoelectronic and biomedical applications. To initiate a nano-silicon revolution, great advancements in size-separation techniques for use with ncSi are required in order to isolate and study these monodisperse fractions. Here we introduce density gradient ultracentrifugation (DGU) as a straightforward experimental method for obtaining the first examples of monodisperse fractions of ncSi.

DGU is a size-separation technique that has been studied extensively over the past decade for purification of single-walled carbon nanotubes (SWNTs) with both aqueous and organic density gradient media.[16,17] For successful separations using DGU, the materials to be separated must have different effective densities that fall within the density extrema of the gradient medium. SWNTs are separated by diameter through adsorption of surfactants or small molecules on their surface, resulting in

Received: May 26, 2011
Published: July 09, 2011

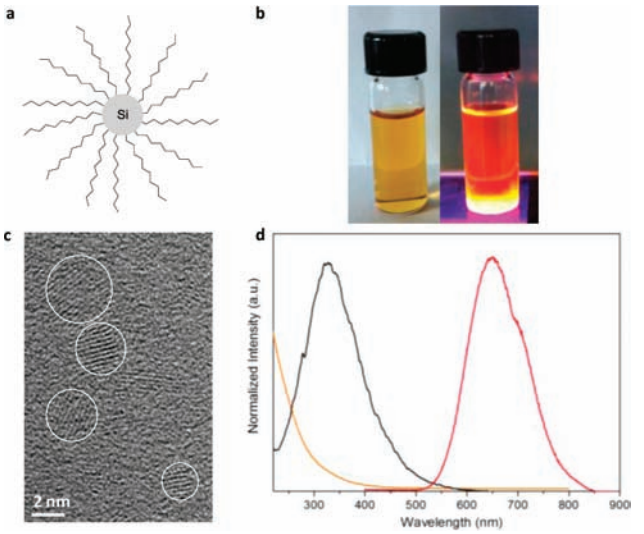

Figure 1. Decyl-capped silicon nanocrystals. (a) Schematic of decyl-capped ncSi. (b) Image of a colloidal suspension of decyl-capped ncSi in hexanes under ambient light (left) and photoexcitation (right). (c) HRTEM image of polydisperse ncSi. (d) UV−vis absorption (orange), PL (red), and excitation (black) spectra of ncSi dispersed in hexanes.

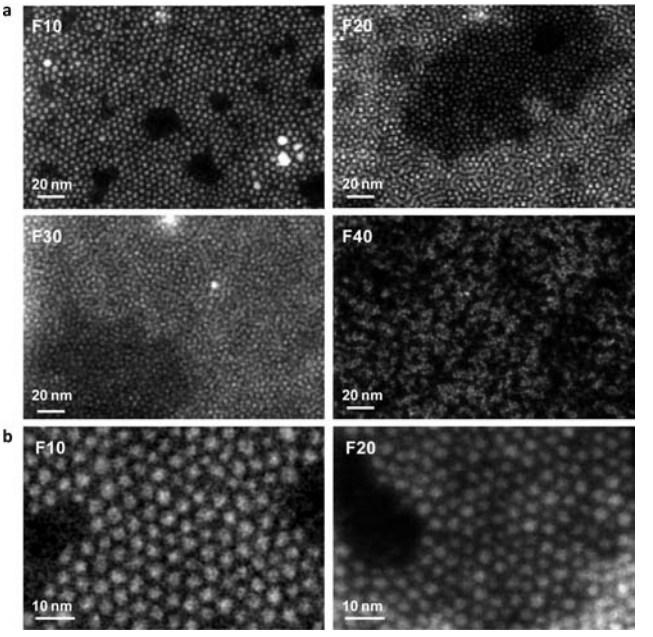

Figure 2. Size analysis of monodisperse ncSi fractions. (a) HAADF-STEM images of fractions 10, 20, 30, and 40 acquired at 300 kV with a nominal spot size of 0.14 nm. (b) Magnified HAADF-STEM images of fractions 10 and 20.

different densities due to their varying surface areas. Surface-functionalized nanoparticles also vary in effective density depending on their size and therefore can be size-separated by DGU. As the ratio of surface area to volume decreases for particles of increasing size, the weighted average of the density of a Si core and surface ligands, for example, results in a higher effective density, since the density of bulk silicon is 2.329 g/cm^3 and the density of organic materials is generally less than 1 g/cm^3. In this manner, successful separations using DGU with surface-ligand-stabilized CdSe, Ag, Au, and FeCo@C nanoparticles have been reported.[18,19] As ncSi are most commonly synthesized with covalently bonded surface organic ligands that provide colloidal stability in solution,[8,9,20−22] they are an ideal candidate for separation by DGU to enable quantification of their size-dependent chemical, physical, and biological properties in subsequent investigations. Here we report the size separation of polydisperse decyl-capped ncSi (ncSi:decyl) using DGU in a self-generated organic density gradient medium.

Throughout this paper, we will refer to nanocrystalline silicon as ncSi, but as we will show and discuss later for our size-separated fractions, the structure of the Si core may change from one with the periodic diamond lattice of bulk Si to another that appears amorphous or molecular, perhaps diagnostic of the fuzzy regime between nanoscale crystalline and cluster Si.

Hydride-terminated ncSi were synthesized using a previously reported method involving high-temperature thermal processing of sol−gel hydridosilicate ($HSiO_{1.5}$) glasses derived from trichlorosilane ($HSiCl_3$) followed by etching with HF to liberate the ncSi from the encapsulating SiO_2 matrix.[23] The resulting hydride-capped ncSi were functionalized with decyl chains (Figure 1a) using a thermally initiated hydrosilylation reaction with 1-decene to produce a stable colloidal dispersion. The purified ncSi:decyl were dispersed in hexane or toluene, resulting in a clear orange solution displaying bright orange-red PL under photoexcitation at 365 nm (Figure 1b).

The as-prepared polydisperse ncSi:decyl were extensively characterized [Supporting Information (SI) Figures 1−5] and consist of a crystalline Si core and extensive alkyl surface termination with limited (although not negligible) surface oxidation. This high degree of alkyl surface coverage provides the present ncSi with excellent colloidal stability, a key requirement for DGU separations. High-resolution transmission electron microscopy (HRTEM) imaging of the ensemble (Figure 1c) shows spherically shaped nanocrystals with a lattice spacing of 0.31 nm, consistent with the (111) lattice spacing of diamond-structure crystalline silicon. An average diameter of ca. 3.2 nm was measured by HRTEM (n = 100, σ = 0.7 nm), and the as-prepared sample was found to have considerable polydispersity (22%). The absorption spectrum (Figure 1d) shows an onset at ca. 500 nm that gradually rises into the UV. The PL spectrum is characterized by a single broad emission band centered at 650 nm and a single broad excitation maximum at 325 nm. The significant line width of the PL spectrum is attributed partly to inhomogeneous broadening from the distribution of nanocrystal sizes as measured using HRTEM.

A previously reported single-step DGU method was used for the size separation of the polydisperse ncSi ensemble.[17] This method exploits the redistribution of a heavy organic additive during ultracentrifugation to form a self-generated density gradient, simultaneously separating materials of varying density in a single step. Typically, 2 mL of ncSi dispersed in toluene was overlaid onto 6 mL of 40 wt % 2,4,6-tribromotoluene in chlorobenzene as the density gradient medium (see the SI for complete experimental details). Following ultracentrifugation, a yellow-colored region evolved within the density gradient medium, corresponding to ncSi:decyl organized by density and size. A small amount of brown solid precipitated at the bottom of the centrifuge tube, representing ncSi with densities larger than the maximum density of the gradient. As discussed below, this precipitated fraction is primarily composed of the larger, most crystalline particles in the ensemble. Fractions of ca. 150 μL of

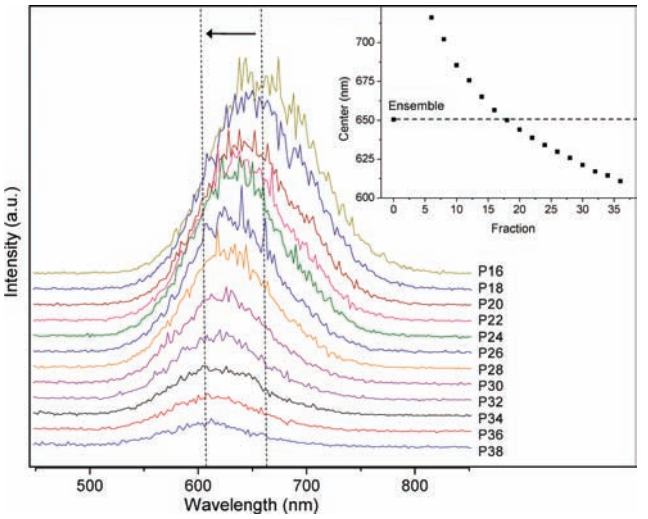

Figure 3. PL spectra of ncSi fractions extracted from fluorescence maps at 345 nm for different DGU fractions. The inset shows the wavelength of the peak center of the DGU fraction plotted against the fraction number, summarizing the blue shift in PL observed with increasing fraction number.

the density gradient solution were collected by carefully puncturing the tube at the top and bottom and applying a slight air overpressure via the top hole.

Following DGU, selected isolated fractions were imaged with high-angle annular dark-field scanning transmission electron microscopy (HAADF-STEM). *Z*-contrast HAADF-STEM images of fractions 10, 20, 30, and 40 (Figure 2a) show a dramatic decrease in particle size with increasing fraction number (lower density), consistent with previous reports on DGU separations of organically capped nanoparticles[17,18] and indicating that the ncSi were successfully separated into fractions of different sizes. All of the HAADF-STEM images show a collection of particles of substantial monodispersity, as observed qualitatively from the hexagonal ordering visible in the images of fractions 10 and 20 in particular (Figure 2b). Particle size statistics were obtained for fractions 10, 20, and 30 at higher magnification (SI Figure 6); the measured average diameters were 2.2, 1.5, and 1.3 nm and the polydispersity index (PDI) values were 1.04, 1.05, and 1.06, respectively.

Surprisingly, HRTEM images of fractions 10, 20, and 30 (SI Figure 7) show lattice fringes for only a limited number of larger particles in fractions 10 and 20, suggesting that the majority of the smaller particles in fractions 10, 20, 30, and 40 were not crystalline. It is important to note that the largest particles in the as-prepared sample, which were crystalline as established by powder X-ray diffraction, precipitated to the bottom of the DGU centrifuge tube and therefore are not included in these images. The observation of ncSi lattice fringes by HRTEM has been reported for ncSi:OR synthesized by $SiCl_4$ reduction, showing a cubic diamond structure for diameters greater than 1.5 nm and a different crystalline structure for particles as small as 1.1 nm.[24] Despite the fact that the present instrument and sample purity were sufficient to obtain comparable results, we observed lattice fringes by HRTEM only for particles larger than 2.5 nm in both the fractionated and ensemble ncSi samples. Selected-area electron diffraction (SAED) experiments (SI Figure 8) were also consistent with the lack of crystallinity observed in the HRTEM images of the fractions. Only fraction 10 showed a weak ring pattern for crystalline silicon, and fractions 20, 30, and 40 did not show any noticeable reflections attributable to crystalline Si. One explanation for the lack of crystallinity is that we observed a transition from the nanocrystal (ncSi:R) to nanocluster (Si_nR_n) size regime across the fuzzy interface between molecular and quantum-size-effect nanomaterials. Another possibility is that we observed a nanocrystalline to nanoamorphous transition. The lack of crystallinity observed in these small Si particles fractioned by DGU is the topic of a continuing investigation.

PL spectra were acquired for various fractions obtained at an excitation wavelength of 345 nm (Figure 3). Each spectrum shows a broad peak centered at 600−650 nm, with the peaks shifting to higher energy with increasing fraction number (i.e., with decreasing size). The striking monotonic increase in the PL energy (blue shift) with increasing DGU fraction number and decreasing ncSi size is consistent with quantum-size effects expected for ncSi:R smaller than the 5 nm exciton size of bulk silicon and indicates that all of the fractions are indeed ncSi and not some adventitious contaminant. It is also interesting to consider this smooth PL shift in light of the lack of crystallinity previously mentioned. The results provide some of the strongest evidence that we have indeed achieved the stated objective, namely, successful separation of ncSi:R on the basis of density and hence size, and that the collected fractions can be used to quantify the size-dependent properties of ncSi:R. The PL data also supplement the evidence that the ncSi become more monodisperse with fractionation by DGU, as indicated by the change in line width of the PL spectra due to inhomogeneous broadening. The PL full width at half-maximum of the fractioned samples (summarized in SI Figure 9) is smaller than that of the ensemble sample and appears to increase with decreasing particle size, which is consistent with the PDI values calculated for fractions 10, 20, and 30, suggesting that some fractions have more polydispersity than others.

Overall, our results indicate that we have separated and isolated ncSi:decyl fractions with considerable monodispersity relative to the initial ensemble sample using a straightforward one-step DGU method. Further improvement in the monodispersity of our ncSi:decyl fractions may be achieved by considering the surface coverage and presence of surface oxides, which can result in a density difference for particles of identical size. Alkyl-capped nanocrystals of uniform crystal size should have the same overall particle size; however, in the presence of surface oxidation, repulsive forces between the oxide species and adjacent alkyl chains may alter the packing of the surface groups, varying the overall particle size, capping-layer density, and effective density of the particle. In his recent review, Shirahata suggests a correlation between a low molecular packing density of hydrocarbon chains and oxidation on the ncSi surface, noting a similarity between FTIR C−H stretches reported for ligand-capped ncSi with oxides and monomolecular films with disordered hydrocarbon chains.[25] These reported C−H stretches associated with disordered hydrocarbon packing are close to the antisymmetric and symmetric vibrations of 2922 and 2850 cm^{-1} observed in the FTIR spectrum of the ncSi:decyl ensemble sample (SI Figure 5), indicating that there may be some degree of disorder in the packing of the surface groups due to the presence of trace surface oxides. Varying degrees of oxidation may also be observed for particles of different size as a result of surface curvature. On low-curvature crystals, steric repulsion between ligand tails prevents ligands from binding

closely together at the surface, leaving a large number of Si−H sites open for oxidation in comparison with high-curvature crystals, which allow more space for the ligand tails. However, the high ligand density associated with particles of low curvature has been reported to shield the surface from reaction with small molecules,[26] indicating that oxide species may be able to reach the surface of smaller nanocrystals more easily. The increase in PDI of fractions with decreasing size may be due to an increased presence of surface oxidation, but in order to quantify this potential trend, further study of the relationship between the extent of oxidation and the crystal size is required.

The minimal polydispersity observed for the collected ncSi:decyl fractions may also be the result of varying crystallinity of the particle cores. Amorphous silicon has been reported to have a density between 70 and 100% of that for crystalline silicon, depending on the preparation conditions.[27] Nanoamorphous silicon particles or Si_nR_m nanoclusters having a lower density than ncSi:R would be consistent with the HRTEM results showing only crystalline particles in the fractions of higher density. A difference in density arising from varying core crystallinity and surface oxidation, as well as size, would allow the particles to be separated by DGU into fractions of varying size and structural composition, similar to work reported for CdS nanorods by Ma et al.[28] Further optimization of the DGU separation parameters (i.e., separation time, density gradient, centrifuge speed) or additional DGU separation steps should allow for the isolation of ncSi species with uniform structural composition for further analysis, which we intend to use for our continuing investigations of the crystallinity of the ncSi core and the extent of surface oxidation relative to crystal size.

In this preliminary study, we have shown that size separation of polydisperse ncSi:decyl can be achieved using DGU, affording monodisperse ncSi fractions of varying size as characterized by HAADF-STEM and PL spectroscopy. Monodisperse ncSi:decyl samples were fractionated in a one-step DGU process and can easily be separated from the density gradient medium. DGU is a useful technique that will prove to be invaluable for the quantification of the size-dependent structural, optical, electrical, and biological properties of silicon. The size dependence of the properties of ncSi is crucial to the development of property-specific ncSi optoelectronic and biomedical applications, as is the ability to make monodisperse ncSi fractions of varying size for the construction of uniform assemblies for state-of-the-art devices.

■ ASSOCIATED CONTENT

Supporting Information. Experimental details and additional characterization of the ncSi ensemble and fractions. This material is available free of charge via the Internet at http://pubs.acs.org.

■ AUTHOR INFORMATION

Corresponding Author
gozin@chem.utoronto.ca

■ ACKNOWLEDGMENT

G.A.O. is a Government of Canada Research Chair in Materials Chemistry. He is deeply indebted to the Natural Sciences and Engineering Council (NSERC) of Canada for strong and sustained support of his research and thanks the Ministry of Science, Research and the Arts of Baden-Wurttemberg's International Guest Professorship Program for financial support of this work. This work was partially carried out with the support of the Karlsruhe Nano Micro Facility, a Helmholtz Research Infrastructure at Karlsruhe Institute of Technology. E.H. and M.M. are grateful for scholarships from NSERC, and F.M.F. acknowledges generous support from the Karlsruhe School of Optics and Photonics.

■ REFERENCES

(1) Talapin, D. V.; Lee, J. S.; Kovalenko, M. V.; Shevchenko, E. V. *Chem. Rev.* **2010**, *110*, 389.
(2) Colvin, V. L.; Schlamp, M. C.; Alivisatos, A. P. *Nature* **1994**, *370*, 354.
(3) Chan, W. C. W.; Nie, S. *Science* **1998**, *281*, 2016.
(4) Michalet, X.; Pinaud, F. F.; Bentolila, L. A.; Tsay, J. M.; Doose, S.; Li, J. J.; Sundaresan, G.; Wu, A. M.; Gambhir, S. S.; Weiss, S. *Science* **2005**, *307*, 538.
(5) Kirchner, C.; Liedl, T.; Kudera, S.; Pellegrino, T.; Javier, A. M.; Gaub, H. E.; Stölzle, S.; Fertig, N.; Parak, W. J. *Nano Lett.* **2005**, *5*, 331.
(6) Derfus, A. M.; Chan, W. C. W.; Bhatia, S. N. *Nano Lett.* **2004**, *4*, 11.
(7) Canham, L. T. *Appl. Phys. Lett.* **1990**, *57*, 1046.
(8) Liu, S. M.; Yang, Y.; Sato, S.; Kimura, K. *Chem. Mater.* **2006**, *18*, 637.
(9) Pi, X. D.; Liptak, R. W.; Deneen Nowak, J.; Wells, N. P.; Carter, C. B.; Campbell, S. A.; Kortshagen, U. *Nanotechnology* **2008**, *19*, No. 245603.
(10) Zou, J.; Sanelle, P.; Pettigrew, K. A.; Kauzlarich, S. M. *J. Cluster Sci.* **2006**, *17*, 565.
(11) Krueger, K. M.; Al-Somali, A. M.; Falkner, J. C.; Colvin, V. L. *Anal. Chem.* **2005**, *77*, 3511.
(12) Murray, C. B.; Norris, D. J.; Bawendi, M. G. *J. Am. Chem. Soc.* **1993**, *115*, 8706.
(13) Anand, M.; Odom, L. A.; Roberts, C. B. *Langmuir* **2007**, *23*, 7338.
(14) Shirahata, N.; Hirakawa, D.; Sakka, Y. *Green Chem.* **2010**, *12*, 2139.
(15) Alsharif, N. H.; Berger, C. E. M.; Varanasi, S. S.; Chao, Y.; Horrocks, B. R.; Datta, H. K. *Small* **2009**, *5*, 221.
(16) Arnold, M. S.; Stupp, S. I.; Hersam, M. C. *Nano Lett.* **2005**, *5*, 713.
(17) Stürzl, N.; Hennrich, F.; Lebedkin, S.; Kappes, M. M. *J. Phys. Chem. C* **2009**, *113*, 14628.
(18) Bai, L.; Ma, X.; Liu, J.; Sun, X.; Zhao, D.; Evans, D. G. *J. Am. Chem. Soc.* **2010**, *132*, 2333.
(19) Sun, X.; Tabakman, S. M.; Seo, W. S.; Zhang, L.; Zhang, G.; Sherlock, S.; Bai, L.; Dai, H. *Angew. Chem., Int. Ed.* **2009**, *48*, 939.
(20) Hua, F.; Swihart, M. T.; Ruckenstein, E. *Langmuir* **2005**, *21*, 6054.
(21) Pettigrew, K. A.; Liu, Q.; Power, P. P.; Kauzlarich, S. M. *Chem. Mater.* **2003**, *15*, 4005.
(22) Buriak, J. M. *Chem. Rev.* **2002**, *102*, 1271.
(23) Henderson, E. J.; Kelly, J. A.; Veinot, J. G. C. *Chem. Mater.* **2009**, *21*, 5426.
(24) Shirahata, N. *Phys. Chem. Chem. Phys.* **2011**, *13*, 7284.
(25) Shirahata, N.; Hasegawa, T.; Sakka, Y.; Tsuruoka, T. *Small* **2010**, *6*, 915.
(26) Mei, B. C.; Oh, E.; Susumu, K.; Farrell, D.; Mountziaris, T. J.; Mattoussi, H. *Langmuir* **2009**, *25*, 10604.
(27) *Properties of Amorphous Silicon*, 2nd ed.; INSPEC: London, 1989.
(28) Ma, X.; Kuang, Y.; Bai, L.; Chang, Z.; Wang, F.; Sun, X.; Evans, D. G. *ACS Nano* **2011**, *5*, 3242.